

# Dependence of the energy confinement on plasma edge radiation cooling in T-10

Razumova K.A., Kasyanova N.V., Gorbunov E.P., Dremin M.M., Kislov A.Ya., Kluchnikov L.A., Krupin V.A., Krylov S.V., Lysenko S.E., Myalton T.B., Nemets A.R., Notkin G.E., Nurgaliev M.R., Sarychev D.V., Sushkov A.V., Chistyakov V.V.

*NRC "Kurchatov Institute", Moscow, Russia*

## 1. Introduction

Enhancement of the energy confinement due to edge radiation cooling has a great importance for future fusion reactor ITER. This effect has been studied in different tokamaks for decades [1] but its causes are not yet entirely understood. In most experiments Ne was used as a radiating gas. It is well known that Ne has the gas recycling ratio close to unity and relatively high radiation losses with a small increase in plasma density. This allows us to separate two possible origins of the confinement improvement: the density value itself and the intensity of radiation cooling. In this work, the energy confinement improvement during impurity gas puffing in the T-10 tokamak is studied. The main purpose of the work is to clarify whether the well-known effect of the  $\tau_e$  improvement with  $n_e$  is really linked with the plasma density level or with the inevitable accompanying process of the edge radiation cooling during the puffing of the working gas.

## 2. Experiments with impurity gas puffing

Experiments were carried out in the T-10 tokamak (major radius  $R = 1.5$  m, minor radius  $a = 0.3$  m) in discharges with plasma current  $I = 220$  kA and toroidal magnetic field  $B = 2.3$  T. A gyrotron with a frequency of 129 GHz was used for on-axis electron cyclotron resonance heating (ECRH). The ECRH power  $P_{EC}$  was varied from 400 to 900 kW. In addition to the usual valve for the working gas injection, the "fast" valve (located close to the plasma) was used for He or Ne puffing. It was opened for one-two ms either in the OH (Ohmic heating) phase or in the stationary phase with ECRH. The time evolution after the impurity gas puffing may be divided into two phases: during the first 15 – 20 ms the plasma is cooled-down up to a minor radius between 18 – 20 cm. Then the temperature profile  $T_e(r)$  is restored and becomes stationary. In this phase the impurity gas is supplied from the wall and the limiters due to recycling. We will analyze the processes in the second stationary phase. Figure 1 shows the temporal behaviour of the stored energy  $W_{dia}$  in an experiment with on-axis heating by one gyrotron ( $P_{EC} = 400 – 450$  kW) and Ne puffing during the steady state phase of ECRH. It is

clearly visible that the stored energy increases by a factor of two when the puffing of the radiating gas increases. Figure 2 shows the results of experiments with He puffing. In both cases (Ne and He) the stored energy  $W_{\text{dia}}$  and the electron density increase. Note that although He and Ne cool the plasma in different radial zones, an essential difference in confinement improvement is not observed. Figure 3 shows the results of experiments with different initial density. In shots #65690 and #65691 the  $\text{D}_2$  puffing was switched-off before the Ne injection. The increase in the density  $\Delta n_1$  for the pair of shots #65691 #65692 is substantially less than the density increase  $\Delta n_2$  for shots #65689 and #65690 with a lower initial density, although the Ne influx in these shots was about 1.5 times higher. Hence, the  $n_e$  increase in shot #65690 is resulting from the confinement improvement rather than from the ionization of the impurity gas. Figure 4 shows the results of experiments, in which the puff of the working gas is not switched-off but the amount of injected Ne is varied (shots ## 65063 – 65075). Ne injection started 100 ms after the start of ECRH. The stored energy  $W_{\text{dia}}$  is plotted as a function of the average plasma density (figure 4(a)) and the total radiation losses  $P_{\text{rad}}$  (figure 4(b)). In figure 4(a) we see a set of points scattered in a vertical direction; while in figure 4(b) the dependence is similar to that shown in inset; i.e.  $W_{\text{dia}}$  increases and then saturates at high radiation losses. As an example, we selected three points with different stored energy  $W_{\text{dia}}$  among the cloud of points in figure 4(a) and marked them by large symbols. We see that these points lay on the single curve in figure 4(b). Thus, we can conclude that  $\tau_E$  depends on  $P_{\text{rad}}$ , but does not depend on the density  $\bar{n}_e$ .

### 3. Analysis of the experimental data

In this work, the explanation of the observed effect is offered from the position of plasma self-organization. Possible reason for the energy confinement enhancement is a reduction of the transport coefficient while the radial thermal flux decreases, as it has been shown in [3]. To describe the experimental data the energy balance equation obtained in [4] from Smoluhovskiy's equation was used:  $\frac{\partial p}{\partial t} = \nabla \left[ \frac{\theta p}{\xi} \nabla \ln(p/p_c) \right]$ , (1)

here the thermal flux density is  $\Gamma = -\theta/\xi (\nabla p + p \nabla \ln(p/p_c))$ ;  $p$  is the plasma pressure;  $k_0 = 1/p_c \cdot dp_c/dr$  is the normalized derivative of the self-consistent pressure profile  $p_c$ ;  $\theta \propto p_0 \beta / q_L \propto p_0^2 / (B_0^2 q_L)$  characterizes some energy strength of the system;  $\xi$  is the dissipation factor depending on the turbulent transport mechanisms. So,  $\theta/\xi$  has the dimensionality of the diffusivity. Using equation (1) it is possible to estimate the increase in the transport coefficient  $\theta/\xi$  at the plasma edge needed to describe the energy confinement enhancement observed in experiments. We can determine the averaged value of  $\xi$  during the stationary stage before the

plasma edge cooling and its increase in the cooling region after the impurity gas puffing. We assume in our calculations that the increase of the  $\xi$  value is only due to the Ne radiation cooling. The results of the numerical calculations indicate that the transport coefficient  $\theta/\xi$  rises with increase of the radial thermal flux as  $\Gamma^{2/3}$  and additionally depends on the relative change of the thermal flux  $\Delta\Gamma/\Gamma$  due to radiation cooling as shown in Fig. 5. This result allows us to determine the radial dependence of the transport coefficient  $\theta/\xi$ . In Fig. 6 is shown the transport coefficient  $\frac{\theta}{\xi} = c_0 + c_1 \frac{\Gamma^{2/3}}{(1 - \frac{\Delta\Gamma}{\Gamma})}$  (here  $c_0 = 0.02 \text{ m}^2\text{s}^{-1}$ ,  $c_1 = 0.29 \text{ m}^{10/3}\text{s}^{-1}\text{kW}^{-2/3}$ ) as a function of normalized minor radius  $r/a$  for shot #65077. Note that  $\theta/\xi$  decreases with the minor radius.

#### 4. Conclusions

1) The well-known dependence of the energy confinement time on the plasma density ('Alcator scaling') turns out to be a dependence on the radiation loss intensity at the plasma edge, which always accompanies puffing of the main working gas. 2) The effect of the energy confinement enhancement with the radiation cooling of the plasma edge can be explained as a reduction of the transport coefficient while the radial thermal flux decreases. 3) The dependence of the transport coefficient on the value of thermal flux is estimated from the experimental data using the energy balance equation for the self-organized plasma (1).

This work was supported by Rosatom (State Contract №H.4x.44.9b.16.1021 of 28.03.2016).

#### References

- [1] Onsgaard J *et al* 1999 Plasma Phys. Control. Fusion **41** A379
- [2] Esipchuk Yu V *et al*. 2003 Plasma Phys. Control. Fusion **45** 793
- [3] N.Timchenko, K.Razumova *et al*. Proc. 41<sup>st</sup> EPS Conf. on Plasma Physics, 2014, ECA, vol.38F, P4.056
- [4] K.S. Dyabilin, K.A. Razumova, Nucl. Fusion 55 (2015) 053023

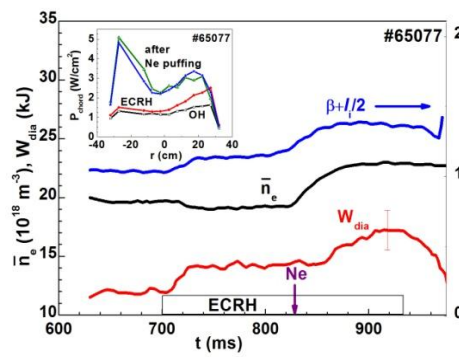


**Fig. 1.** On-axis ECRH with Ne puffing. Temporal behaviour of  $\beta_p + l_i/2$  ( $l_i$  is the internal inductance); line average density  $n_e$  and the stored energy  $W_{dia}$  with the systematic error. Inset shows radiation losses measured along vertical chords.

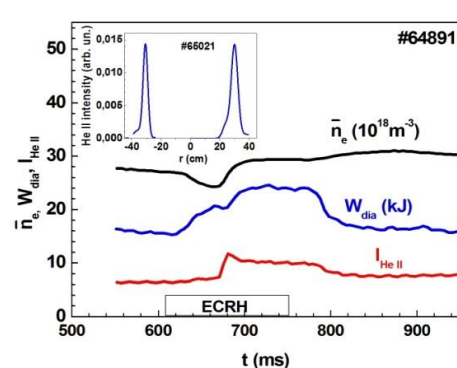


**Fig. 2.** On-axis ECRH with He puffing. Temporal behaviour of the line average density  $n_e$ , stored plasma energy  $W_{dia}$  and He II line intensity. Inset shows radial distribution of the He II line intensity after Abel inversion for the shot with He puffing.

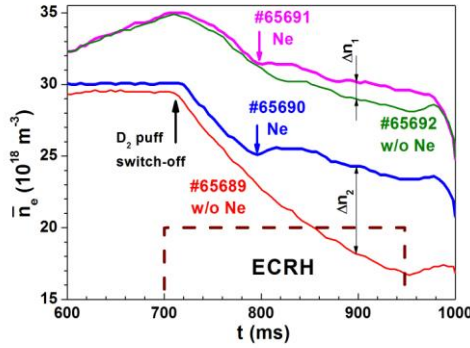


**Fig. 3.** The density evolution in shots with different initial density, with and without Ne puffing. In shot #65691 the Ne puffing intensity is 1.5 times higher than in #65690. The deuterium valve was switched-off before the Ne puffing.

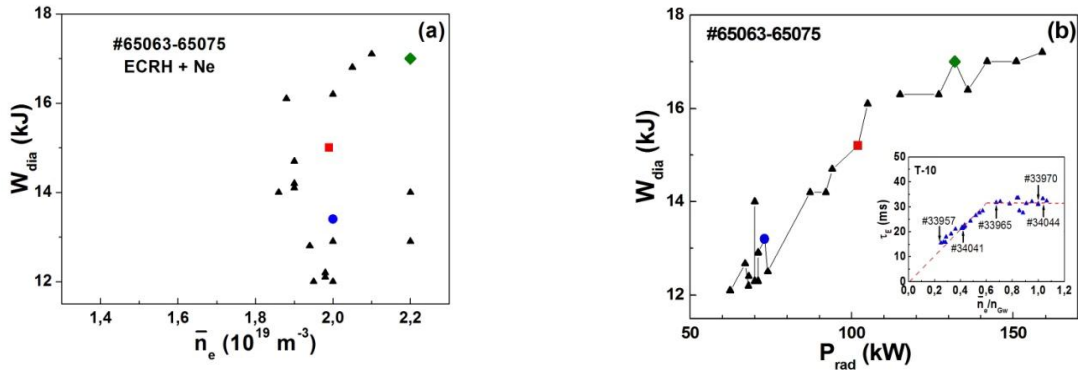


**Fig. 4.** Shots with Ne puffing in pure OH and on-axis ECRH heated discharges; (a) shows the large scatter in the stored energy  $W_{\text{dia}}$  as a function of the density  $n$ , while (b) shows the functional dependence for the same discharge data on the radiated power. Three typical selected points marked by large symbols also demonstrate that dependence of stored energy on density should be replaced by dependence on the radiation power. Inset shows the typical dependence of the energy confinement time on the plasma density normalized to the Greenwald density [2].

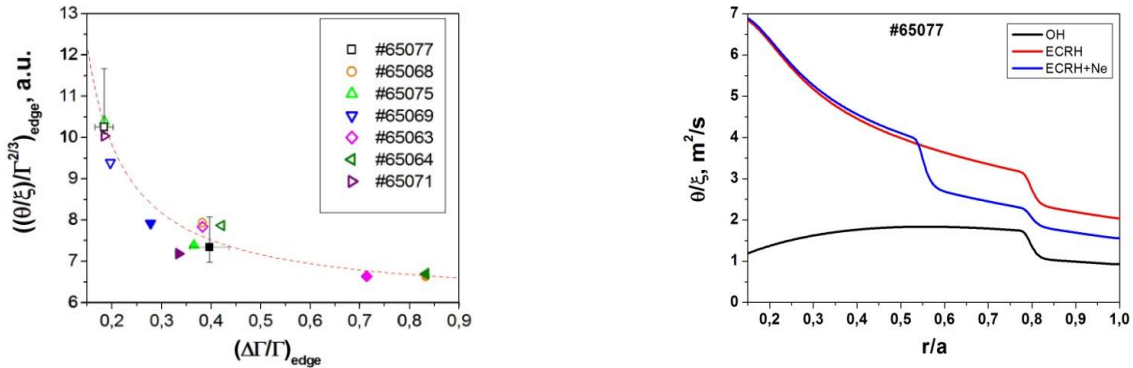


**Fig. 5.** Calculated dependence of value  $\frac{\theta/\xi}{\Gamma^{2/3}}$  on relative flux change  $\Delta\Gamma/\Gamma$  near the plasma edge. Results before and after Ne puffing are represented by open and full symbols, respectively. Horizontal error bars correspond to uncertainty up to 15% in radiated power, while vertical bars correspond to estimated uncertainty in  $W_{\text{dia}}$ .

**Fig. 6.** Radial dependence of the transport coefficient for three stationary stages of discharge #65077 (with OH and ECRH before and after Ne puffing).